A Fast Linear Reconstructor for the Nonlinear Curvature Wavefront Sensor (nlCWFS)

Johanan L. Codona[1], Mala Mateen[2], and Michael Hart[1]
[1]Hart Scientific Consulting International, LLC, 2002 N. Forbes Blvd. #102, Tucson, AZ 85745
[2]Air Force Research Laboratory, Kirtland AFB, NM 87117

ABSTRACT

The Nonlinear Curvature Wavefront Sensor (nlCWFS), first proposed by Guyon,[1] determines wavefront shape from images of a reference beacon in a number of "Fresnel planes" between the pupil and focal plane of a telescope. We previously described a fast linear algorithm[2] that used refractive strong scintillation theory as an inspiration to use appropriately smoothed or binned Fresnel plane images to recover low spatial frequency aberrations. Since a given aberration causes both linear and nonlinear irradiance variations, we had suggested that the linear method be used to estimate the larger aberrations and that an unspecified nonlinear algorithm be used to estimate the nonlinear residual. In this paper we show that while there is always a nonlinear residual, if we only use the linear algorithm in a closed loop AO system, the nonlinear residual will never be an important term in the error budget. This greatly simplifies the nlCWFS system concept, allowing a closed-loop AO system to be driven from a linear algorithm operating on images from a selection of Fresnel plane cameras. The relationship between a localized variation in the irradiance and the pupil phase has a spatial frequency structure that can be used to select the Fresnel planes. The required number of Fresnel planes increases with D/r_0. The required image processing can be parallelized per-camera, including binning, spatial moments, normalization, and contributions to the estimated wavefront.

Keywords: Adaptive Optics; Wavefront Sensing; Nonlinear; Curvature.

1. INTRODUCTION

The *Nonlinear Curvature Wavefront Sensor* (nlCWFS)[1,3] determines the pupil plane wavefront aberrations by examining the irradiance from a beacon in a number of defocused image planes located between the pupil and focal plane of a telescope. Since the irradiance patterns have structure at the full diffraction limit of the telescope and use light from the entire pupil, it is possible to obtain very high accuracy and efficiency. The potential advantages of the technique are independent of the algorithm used for extracting the wavefront from the images, so long as all of the diffraction-limited information is included. To accurately estimate the pupil plane aberrations responsible for a particular set of images, an iterative nonlinear wavefront retrieval algorithm is commonly used[1,3], which is presently too slow to be used in an astronomical adaptive optics (AO) system.

Noting that the Fresnel scale ($R_f = \mathrm{sqrt}(\lambda z)$ for an infinite focal length, where z is the distance to the pupil plane) runs from 0 at the pupil to infinite at the focal plane, any amount of phase aberration will lead to strong scintillation within the telescope, unless it is limited by the pupil mask. Strong scattering can be described as when aberrations due to the medium (characterized by the Fried length r_0) dominate geometric effects such as the difference between plane waves and spherical waves at a particular range (characterized by the Fresnel scale), or $r_0 < R_f$. A feature of strong scattering is the appearance of larger-scale irradiance structure that refractively focuses the light over a region of approximately $z\theta_0 = z(\lambda/r_0)$, which modulates the smaller-scale scintillation patterns with spatial scales characterized by r_0. We previously suggested[2] that the Fresnel plane images minus the average intensity be smoothed (or binned) to better isolate the refractive scintillation and then linearly relate the delta-irradiance pixels to the pupil aberrations to the aberrations using random test aberration patterns. The result was similar to linear curvature wavefront sensing, but with a more complicated relationship between the wavefront and the irradiance fluctuation. There is always a nonlinear residual, so we previously considered including a nonlinear final wavefront estimation step that could possibly be simpler due to the not having to deal with the full amount of the wavefront aberrations.

In this paper we show that when used to correct atmospheric aberrations in an adaptive optics closed loop, the portion of the wavefront error (WFE) that is correctly estimated by the linear algorithm reduces the residuals until they eventually

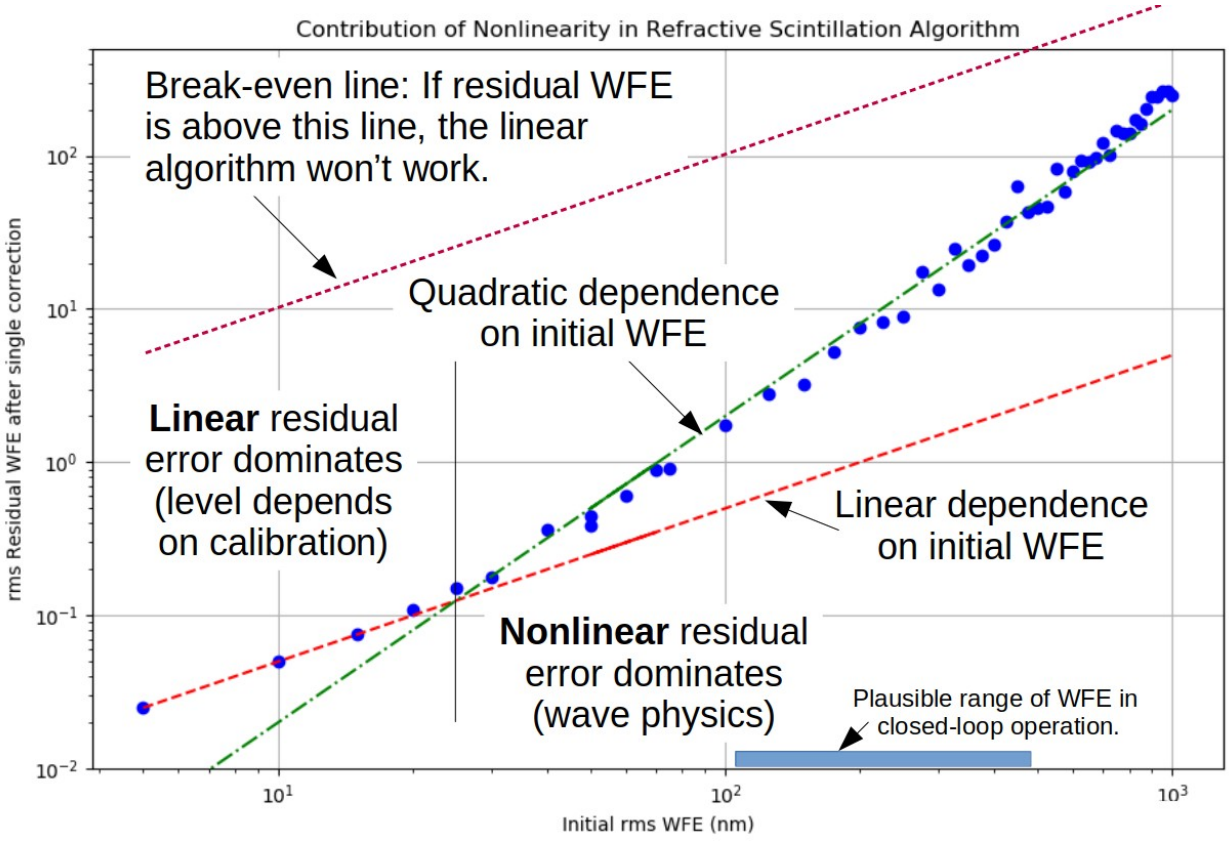

Figure 1. *This shows the estimated residual WFE after subtracting the result of the linear algorithm, as a function of starting WFE. The nonlinear contribution to the Fresnel plane irradiance increases with greater WFE, leaving us with a greater residual error that does not follow the linear model.*

become less than the nonlinear residuals, at which point they are quite small. However, for typical astronomical telescopes and atmospheric conditions, other sources of error dominate and there is no point at which the nonlinear residual is dominant. This brings us to the conclusion that a nonlinear curvature wavefront sensor could be used with only the approximate linear algorithm and still extract the full potential performance of the system. This is entirely due to applying the linear algorithm in a closed loop, which reduces the residuals including the nonlinear portion. It does not imply that this is a viable strategy for accurate wavefront estimation outside of a closed-loop wavefront correction system.

2. THE NONLINEAR CONTRIBUTION TO THE RESIDUAL WFE

In the absence of noise, a "perfect" linear estimator of a system with a linear response to the input will have a zero residual error. Since our reconstructor is estimated from measurements of the full nonlinear irradiance resulting from a test actuator pattern, it will never be "perfect", but will have some systematic linear error. An "imperfect" linear reconstructor will result in a residual WFE that is linearly proportional to the initial WFE. In general, nonlinear physical effects look like "noise" to a linear algorithm. But since the first nonlinear Taylor series correction is second-order, the leading-order nonlinear residual WFE should be at least quadratic in the initial WFE. By examining a scatter plot of initial and single-correction WFE from a numerical experiment, we should see this behavior.

To do this, we simulated a 1m AO-equipped telescope with a 16x16 actuator DM and a 4-camera nlCWFS. The tests used continuous fields to compute the irradiance (i.e. no photon noise), and no other sources of noise were included. We modeled a 1m telescope with an 18mm telescope exit pupil, followed by propagation to 4 Fresnel planes at 6.4 cm, 16 cm, 40 cm, and 100 cm beyond the exit pupil. For the purposes of this analysis, all Fresnel planes were assumed to

use 700 nm light. The example phase screens were synthesized to give an r_0 of 50 cm at 500 nm, which corresponds roughly with the residual WFE that we might achieve in closed loop. Deriving a reconstructor with a more realistic r_0 (or rms WFE with an ordered set of modes) is not recommended since the nonlinearity greatly increases the noise in the training set.

Both the reconstructor training data and the tests were performed using the phase screens to introduce the test aberrations. For the nonlinearity tests, only the correction at the actuator locations was computed, intentionally separating out the effect of fitting error. The test phase screen was sampled at the DM actuator to represent the initial wavefront, while the full resolution of the phase screens was used in creating the incident field and Fresnel plane images. The Fresnel plane images were computed, normalized, and processed into the delta images. The delta-image pixels were then multiplied by the reconstructor matrix to get the estimated actuator values. These were subtracted from the original actuator values and the residual rms WFE was computed. This is repeated with a range of starting WFE values, the results are displayed in Figure 1.

As described above, we expect a linear and quadratic range in the residual WFE. The quadratic portion allows us to estimate the significance of nonlinearities when using the linear reconstruction algorithm. The level of the linear error is a function of the accuracy of the linear reconstructor and is not essential to the physics of the problem. In this case, the linear residual dominates for initial WFE < 25 nm, which is well below a non-extreme AO system's best performance. Even so, an improved reconstructor could be estimated that would leave nonlinear residuals at even lower initial WFE values. The quadratic range resulting from nonlinearity is clearly seen. It is possible to draw a "break-even line" that shows where the WFE before and after are statistically the same. If the initial WFE is worse than this, a single update based on the linear algorithm will make the wavefront error worse. However, this never even comes close to happening over the range of aberrations from uncorrected atmospheric seeing to high Strehl correction. Therefore, we would expect that a nlCWFS AO system will make the correction better with every iteration until until calibration errors or some other source of noise or error stops it. With fairly faint guide stars (say 12th magnitude) and poor seeing with an r_0 of about 5 cm, we might expect a residual WFE of about 200 nm. Even if it were 100 nm, the nonlinear residual error would fall far below it, giving the best possible AO performance without ever having to deal with making a nonlinear wavefront estimate. In an "extreme" AO system, the components are selected to give smaller estimation and fitting errors, along with using brighter guide stars resulting in less photon noise. Even in these situations it is still unlikely that nonlinear wavefront estimates will be needed, and if they were it would appear as a slowdown in the convergence of the closed loop over a limited dynamic range of WFE. This brings us to the surprising conclusion that an AO system can be used with a nlCWFS using only a linear wavefront reconstruction algorithm.

3. PLACING THE FRESNEL PLANES

When designing a nlCWFS, we first need to consider the range of spatial frequencies that we wish to correct, and then decide on the placement of the cameras to give the desired spatial frequency coverage. The relationship can be seen at the actuator resolution by examining the numerically-derived reconstructor. This can be Fourier transformed to linearly relate that spatial spectrum of the wavefront and the Fresnel plane irradiance with a transfer function that varies with spatial frequency κ. We can also derive it in weak scattering directly, giving the PSD transfer function as a transfer function that we could call the Fresnel-Talbot filter

$$\Phi_I(\kappa) = \sin(\kappa^2 \lambda z / 4\pi)\, \Phi_\varphi(\kappa). \qquad (1)$$

This filter gives us the well-known low-spatial-frequency loss of sensitivity, as well as the alternating sign of the Talbot effect, and nulls in the response at certain spatial frequencies. From this we see that having only one Fresnel plane would leave us blind to these spatial frequencies, while two or more planes can still leave blind spots unless we are careful to place them so that we have reasonable coverage over the desired range of spatial frequencies in at least one of the camera images. Considering tip-tilt as corresponding to 1 Fourier cycle/D and focus as 1.5 cycle/D, we need to get information from about 1.5 cycles/D to ($D/2r_{0,science}$) cycles/D for diffraction-limited correction at the science wavelength. The required spatial frequency range is about $D/3r_{0,science.}$ By moving the post-pupil distance of the Fresnel planes, we can try to cover as much of the desired spatial frequency range as possible. An example of this with four cameras is shown in Figure 2. Smaller telescope apertures can require fewer cameras, which further aids in measurement by allowing more wavefront sensor photons to go to each camera.

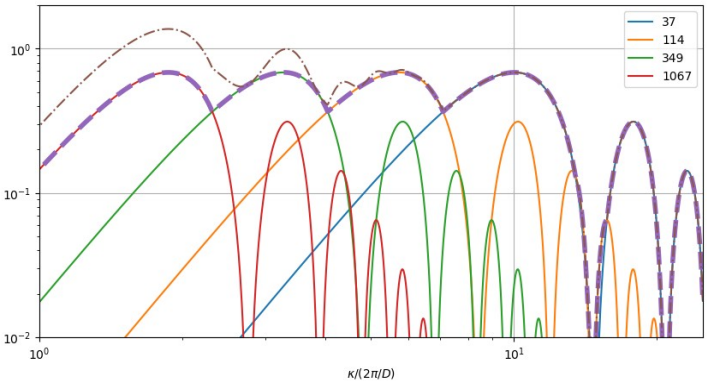

Figure 2*: An example of four camera planes with the Fresnel-Talbot spatial filter shown in a different color for each range. The horizontal axis is in wavefront Fourier cycles/D. The purple dashed curve is the maximum response for that spatial frequency, while the dot-dashed curve is the sum. How deep of a dip in the combined transfer function that can be tolerated depends on the SNR at that spatial frequency, which requires deeper analysis of the particular use case.*

An all-linear processing algorithm for the nlCWFS has the further advantage of being very parallelizable. Each camera can be read, binned, processed, and multiplied by its part of the reconstructor matrix in parallel with the other cameras. Read noise is minimized by optically scaling the camera pixels to match the desired binning size. It shouldn't be necessary to use pixels smaller than the Fried length at the science wavelength. Improved isolation from nonlinearity and lower estimation error noise comes with larger pixels, but greater operational dynamic range comes from smaller pixels. At this point all of the required information is available to design and implement a practical nlCWFS AO system.

4. SUMMARY

We have shown that the linear wavefront estimation algorithm[2] never needs to be supplemented with a nonlinear wavefront estimate to give high-performance AO correction. This will allow processing at speeds that are sufficient to drive a practical real-time AO system. The advantages of the nlCWFS are not due to the nonlinearity, but rather the resolution and light-gathering power of the full aperture. The linear algorithm allows us to use that to our advantage with a simple processing design. We also showed how the Fresnel-Talbot transfer function determines the best placement of the camera planes, as well as how many cameras are required in a particular nlCWFS AO system.

ACKNOWLEDGMENTS

Research supported by AFRL contract FA9451-16-C-0427.

REFERENCES

[1] O. Guyon, "High Sensitivity Wavefront Sensing with a non-linear Curvature Wavefront Sensor," PASP, 122:49-62, 2010.

[2] J. L. Codona, M. Mateen, M. Hart, "A fast wavefront reconstructor for the nonlinear curvature wavefront sensor," Proc. SPIE 10703, Adaptive Optics Systems VI, 107035Q, 2018.

[3] M. Mateen, "*Development and verification of the non-linear curvature wavefront sensor*," Univ of Arizona Dissertation, 2015.